AIAA SciTech
13-17 January 2014, National Harbor, Maryland
55th AIAA/ASMe/ASCE/AHS/SC Structures, Structural Dynamics, and Materials Conference

Modeling of Plain Woven Fabrics for Inflatable Aerodynamic Decelerators

Jeremy L. Hill[1] and Robert D. Braun[2]
Georgia Institute of Technology, Atlanta, GA, 30332-0150

Inflatable Aerodynamic Decelerators (IADs) are often constructed from complex fabrics. The simplest example being a plain woven fabric. Optimization of IADs relies heavily on a detailed understanding of the IAD materials. A Mesomechanical material model of a plain woven fabric is implemented in a nonlinear finite element analysis code and presented in this work. The model is developed in MATLAB to facilitate exploration and learning. Derivation of the model is initially presented by Ivanov and Tabiei and utilizes the homogenization methodology; commonly used in composites. Geometric nonlinearity is modeled through the reorientation, as well as, locking of the yarns. The example shows the mesomechanical material model is capable of capturing the dual behavior corresponding to that of actual plain woven fabrics.

Downloaded by GEORGIA INST OF TECHNOLOGY on January 25, 2014 | http://arc.aiaa.org | DOI: 10.2514/6.2014-0631

Nomenclature

E	=	Elastic Modulus
G	=	Shear Modulus
ρ	=	Mass Density
v	=	Poisson's Ratio
β	=	Undulation Angle
θ	=	Braid Angle
θ_{lock}	=	Locking Angle of Yarns
f	=	Volume Fraction
μ	=	Shear Resistance Discount Factor
q	=	Yarn Unit Direction Vector
F	=	Deformation Gradient Matrix
C	=	Stiffness Matrix

Subscripts

(x,y,z)	=	Yarn Material Coordinate System
(X,Y,Z)	=	RVC Coordinate System
(X',Y',Z')	=	Fabric Coordinate System
N	=	Iso-Strain Components
S	=	Iso-Stress Components
f	=	Fill
w	=	Warp

Acronyms

IAD	=	Inflatable Aerodynamic Decelerator
EDL	=	Entry, Descent, and Landing
RVC	=	Representative Volume Cell

[1] Graduate Research Assistant, Daniel Guggenheim School of Aerospace Engineering, AIAA Student Member.
[2] Professor, Daniel Guggenheim School of Aerospace Engineering, AIAA Fellow.

Copyright © 2014 by the American Institute of Aeronautics and Astronautics, Inc. All rights reserved.

Downloaded by GEORGIA INST OF TECHNOLOGY on January 25, 2014 | http://arc.aiaa.org | DOI: 10.2514/6.2014-0631

I. Introduction

FUTURE space missions will require the landing of larger and heavier payloads on planetary surfaces. As vehicles grow in size, the more difficult it becomes to dissipate all the kinetic energy necessary to meet desired end conditions. Currently, the operating Mach numbers and dynamic pressures of supersonic parachutes, used to decelerate entry vehicles, limit the available payload mass and thereby constrain future mission design. Inflatable Aerodynamic Decelerators (IADs) are a candidate technology NASA began investigating in the late 1960's. Compared to supersonic parachutes, IADs represent a decelerator option that provides a large drag area capable of operating at higher Mach numbers and dynamic pressures[1]. After several decades of little acknowledgement, IADs have seen a resurgence in interest from the Entry, Descent, and Landing (EDL) community in recent years[2]. Technology investments in the last decade have significantly advanced three IAD designs: attached isotensoid, tension cone, and stacked toroid[3,4,5]. A recent attached isotensoid design is shown in Figure 1.

Figure 1: CAD Model of SIAD-E[3]

To date, IAD material modeling has been done on a macroscopic level; treating the fabric as a continuum with isotropic or orthotropic material properties, due to the large complex geometries and complicated loading[6]. More appropriate models exist that do not make the continuum assumption. At the mesoscopic level, the fabric is viewed as a series of interlacing yarns; where the yarns are modeled as a continuum. These models are dependent on individual yarn properties and weave geometry, but determination of these inputs can be difficult and a consistent methodology for IAD applications has yet to be established[7]. In lieu of considering these higher fidelity methods, Murman et al addresses several modeling techniques that can be used to capture some of the complex fabric responses seen on IADs while still utilizing existing model frameworks[8]. Murman and Hutchings both allude to the use of advanced material models for IAD fabrics. However, they also note that detailed modeling of fabrics at the yarn or fiber level is computational intensive and not currently feasible for full-scale IAD modeling.

As part of a broad technology maturation plan, National Full-Scale Aerodynamics Complex (NFAC) wind tunnel testing of the stacked toroid configuration has been carried out to develop design, analysis, manufacturing, and assembly techniques for IADs[5]. To the same end, subsonic rocket sled testing of attached isotensoid and attached torus configurations have been carried out[3]. These experimental tests are used to facilitate comparisons with finite element models. The predictions of finite element models have not always been in close agreement with measured quantities. The complexity of the IADs (e.g. variable boundary conditions, uneven strap loading, load sharing among tori, etc.) makes it very difficult to determine the causes of the differences between the predicted and measured response. Furthermore, IADs and other inflated structures quite often utilize fabrics due to their lightweight and high loading carrying capabilities. Fabrics are complex structures of individual fibers that have been collected into yarns and interlaced together. As an example, the stacked toroid tested in the NFAC consists of a urethane bladder, a braided tube coated with urethane, and axial cords adhered within the braid. Design optimization of these inflated structures relies on a detailed understanding of the fabric mechanics.

Outside the IAD community, there are several approaches for modeling fabrics and their effective properties. Due to computational expense, most methods consider the smallest repeating pattern that can properly represent the fabric under loading conditions; usually termed the unit cell[9]. Peng utilizes a novel approach for predicting the effective nonlinear elastic moduli of a fabric; in which a unit cell was built and, by varying the loading and boundary conditions, numerical tests similar to uniaxial tension testing and shear frame testing were carried out. The results are imposed on a four node shell element that can be applied to large scale model[9]. Shell elements are desirable for modeling inflatable structures due to contact and transverse pressure loading. The model utilized in this work has been implemented in the nonlinear dynamic explicit finite element code, LS-DYNA, by Tabiei and Ivanov[10]. This work intends to implement the model in MATLAB within a simple nonlinear static analysis code in an effort to gain experience and enable a greater degree of examination for proper behavior.

II. Mesomechanical Model

The development of this model follows the derivations of Ivanov and Tabiei. A representative volume cell (RVC) is utilized for this work. The plain woven fabric is shown in Figure 2 along with the boundary of the RVC. The RVC is constructed from a rectangular volume in the fabric such that the axes running longitudinal through the yarns intersect the cell corners. This is different than the more common approach; which it to have the mid-sides of the RVC be intersected by the yarn axes[11]. It is assumed that initially the warp and fill yarns are orthogonal; however, as a result of deformations, they will no longer remain orthogonal.

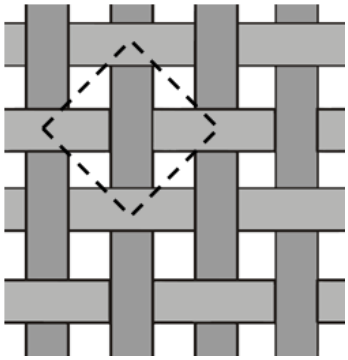

Figure 2: Plain Woven Fabric with Outline of Representative Volume Cell

The RVC is shown in more detail in Figure 3. The RVC is divided into four subcells; as shown on the left. Two of the cells contain the fill yarn and the other two contain the warp yarn. The two subcells containing the same yarn are antisymmetric. The right side of the figure shows the angles utilized for determining the direction of each yarn. The braid angle, θ, and the undulation angle, β. β_f and β_w are defined for the fill and warp yarns, respectively. The subcells are label (*f, w, F,W*), as shown in Figure 3. This will be utilized in the homogenization procedure in an effort to make the mathematical operations clear, as well as take advantage of the antisymmetry.

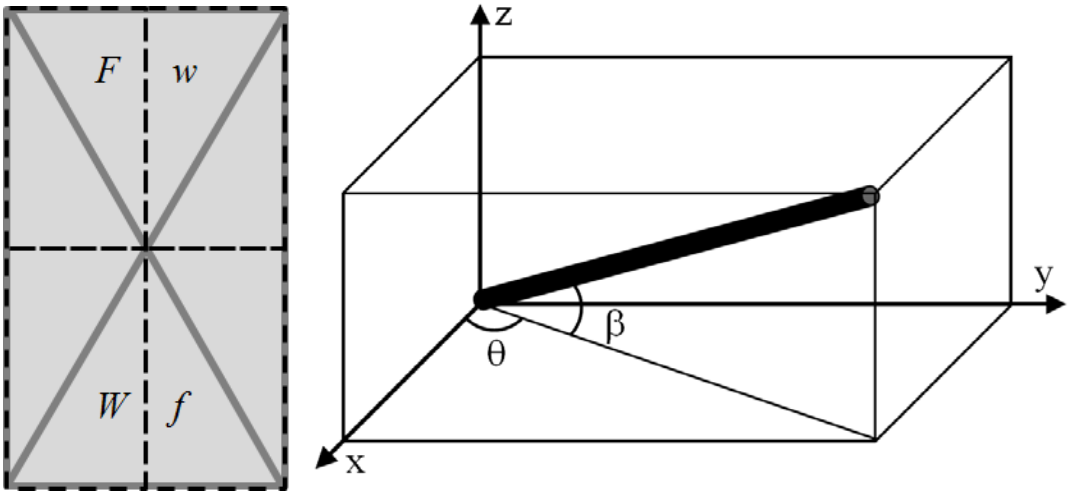

Figure 3: RVC Subcells (Left) and Angles Relating Material and RVC Coordinate Systems (Right)

To begin the homogenization procedure, the various coordinate systems must be defined. Three different coordinate systems will be utilized: the material coordinate system, the RVC coordinate system, and the fabric coordinate system. The material properties of the yarns are expressed in the material coordinate system. The yarns are assumed to be transversely isotropic: meaning a special class of orthotropic material in which it has the same material properties in one plane and different properties in the direction normal to this plane.

The Voigt notation is used to express Hooke's Law. This notation will be consistenly used throughout the development of material model. Equation (1) presents the yarn material stiffness matrix, [*C*], expressed in the material coordinate system is noted with a {″}. The material coordinate axes are labeled with lower case (*x,y,z*). All the coordinate system transformations can be confusing without proper notation.

Downloaded by GEORGIA INST OF TECHNOLOGY on January 25, 2014 | http://arc.aiaa.org | DOI: 10.2514/6.2014-0631

$$\{\sigma''\} = \begin{Bmatrix} \sigma_{xx} \\ \sigma_{yy} \\ \sigma_{zz} \\ \sigma_{xy} \\ \sigma_{yz} \\ \sigma_{xz} \end{Bmatrix} = \begin{bmatrix} C''_{11} & C''_{12} & C''_{13} & 0 & 0 & 0 \\ C''_{21} & C''_{22} & C''_{23} & 0 & 0 & 0 \\ C''_{31} & C''_{32} & C''_{33} & 0 & 0 & 0 \\ 0 & 0 & 0 & C''_{44} & 0 & 0 \\ 0 & 0 & 0 & 0 & C''_{55} & 0 \\ 0 & 0 & 0 & 0 & 0 & C''_{66} \end{bmatrix} \begin{Bmatrix} \varepsilon_{xx} \\ \varepsilon_{yy} \\ \varepsilon_{zz} \\ 2\varepsilon_{xy} \\ 2\varepsilon_{yz} \\ 2\varepsilon_{xz} \end{Bmatrix} = [C''] \begin{Bmatrix} \varepsilon_{xx} \\ \varepsilon_{yy} \\ \varepsilon_{zz} \\ \gamma_{xy} \\ \gamma_{yz} \\ \gamma_{xz} \end{Bmatrix} = [C'']\{\varepsilon''\} \tag{1}$$

The yarn stiffness matrix expressed in the material coordinate system contains 6 elastic constants. E_1, E_2, G_{12}, G_{23}, ν_{12}, and ν_{23} are the Elastic moduli, Shear moduli, and Poisson's ratios of the yarn, respectively. The term in front of the shear moduli, μ, is called the discount factor. It is a function of the braid angle and takes on a value between 0 and 1. The fabric is not a continuous medium and the yarns will rotate over one another until they lock or jam together as a result of being loaded. The discount factor is used to model the low shear resistance in the fabric prior to the locking of the yarns. The initial value of the discount factor is set very close to zero, but due to friction between the yarns, the fabric has some shear resistance. When locking has occurred, it begins to behave as an elastic medium. Thus, the discount factor is set to 1 and the yarn's full shear modulus is regained.

$$[C''] = \begin{bmatrix} \frac{1}{E_1} & -\frac{\nu_{12}}{E_1} & -\frac{\nu_{12}}{E_1} & 0 & 0 & 0 \\ -\frac{\nu_{12}}{E_1} & \frac{1}{E_2} & -\frac{\nu_{23}}{E_2} & 0 & 0 & 0 \\ -\frac{\nu_{12}}{E_1} & -\frac{\nu_{23}}{E_2} & \frac{1}{E_2} & 0 & 0 & 0 \\ 0 & 0 & 0 & \frac{1}{\mu G_{12}} & 0 & 0 \\ 0 & 0 & 0 & 0 & \frac{1}{\mu G_{23}} & 0 \\ 0 & 0 & 0 & 0 & 0 & \frac{1}{\mu G_{12}} \end{bmatrix}^{-1} \tag{2}$$

Different stiffness matrices are used for the fill and warp yarns to allow for the possibility of modeling an unbalanced woven fabric. As part of the homogenization procedure, the yarn material properties expressed in the material coordinate system need to be rotated to the RVC coordinate system. The transformation of each subcell is performed using the following equation. The yarn material stiffness matrix expressed in the RVC coordinate system is noted with a $\{'\}$. $[T]$ is the strain transformation matrix.

$$[C'] = [T(\beta,\theta)]^T [C''][T(\beta,\theta)] \tag{3}$$

This transformation matrix is a function of the directional cosines of the material axes unit vectors with respect to the RVC coordinate system. For purposes of expressing the constitutive matrix of the yarn material in the RVC coordinate system, the following directional cosine convention is followed in the rotation matrix. It should be noted that the components including *sin(β)* have a sign change to treat these rotations as positive rather than negative.

Downloaded by GEORGIA INST OF TECHNOLOGY on January 25, 2014 | http://arc.aiaa.org | DOI: 10.2514/6.2014-0631

$$\begin{Bmatrix} xx \\ yy \\ zz \end{Bmatrix} = \begin{bmatrix} \cos(\beta)\cos(\theta) & \cos(\beta)\sin(\theta) & \sin(\beta) \\ -\sin(\theta) & \cos(\theta) & 0 \\ -\sin(\beta)\cos(\theta) & -\sin(\beta)\sin(\theta) & \cos(\beta) \end{bmatrix} \begin{Bmatrix} XX \\ YY \\ ZZ \end{Bmatrix} = \begin{bmatrix} l_1 & m_1 & n_1 \\ l_2 & m_2 & n_2 \\ l_3 & m_3 & n_3 \end{bmatrix} \begin{Bmatrix} XX \\ YY \\ ZZ \end{Bmatrix} \quad (4)$$

The strain transformation matrix is expressed as follows[12]:

$$[T] = \begin{bmatrix} l_1^2 & m_1^2 & n_1^2 & l_1 m_1 & m_1 n_1 & n_1 l_1 \\ l_2^2 & m_2^2 & n_2^2 & l_2 m_2 & m_2 n_2 & n_2 l_2 \\ l_3^2 & m_3^2 & n_3^2 & l_3 m_3 & m_3 n_3 & n_3 l_3 \\ 2l_1 l_2 & 2m_1 m_2 & 2n_1 n_2 & (l_1 m_2 + l_2 m_1) & (m_1 n_2 + m_2 n_1) & (n_1 l_2 + n_2 l_1) \\ 2l_2 l_3 & 2m_2 m_3 & 2n_2 n_3 & (l_2 m_3 + l_3 m_2) & (m_2 n_3 + m_3 n_2) & (n_2 l_3 + n_3 l_2) \\ 2l_3 l_1 & 2m_3 m_1 & 2n_3 n_1 & (l_3 m_1 + l_1 m_3) & (m_3 n_1 + m_1 n_3) & (n_3 l_1 + n_1 l_3) \end{bmatrix} \quad (5)$$

As a result of expressing the yarn material properties in the RVC coordinate system, the constitutive matrix now has the following form. All of the matrix components are now non-zero. The RVC coordinate axes are labeled with upper case (*X*,*Y*,*Z*).

$$\{\sigma'\} = \begin{Bmatrix} \sigma_{XX} \\ \sigma_{YY} \\ \sigma_{ZZ} \\ \sigma_{XY} \\ \sigma_{YZ} \\ \sigma_{XZ} \end{Bmatrix} = \begin{bmatrix} C_{11} & C_{12} & C_{13} & C_{14} & C_{15} & C_{16} \\ C_{21} & C_{22} & C_{23} & C_{24} & C_{25} & C_{26} \\ C_{31} & C_{32} & C_{33} & C_{34} & C_{35} & C_{36} \\ C_{41} & C_{42} & C_{43} & C_{44} & C_{45} & C_{46} \\ C_{51} & C_{52} & C_{53} & C_{54} & C_{55} & C_{56} \\ C_{61} & C_{62} & C_{63} & C_{64} & C_{65} & C_{66} \end{bmatrix} \begin{Bmatrix} \varepsilon_{XX} \\ \varepsilon_{YY} \\ \varepsilon_{ZZ} \\ \gamma_{XY} \\ \gamma_{YZ} \\ \gamma_{XZ} \end{Bmatrix} = [C']\{\varepsilon'\} \quad (6)$$

Each of the subcell stiffness matrices need to be computed during the homogenization process. Each of the subcells is generally symmetric about the main diagonal. In addition, there is antisymmetry between the fill subcells and the warp subcells. This makes the transformation easier since only two transformations are necessary to calculate all four matrices. The following relation is used to calculate the the *F* subcell stiffness matrix using that of the *f* subcell. The same relation exists between the *W* and *w* subcells.

$$[C^F] = \begin{bmatrix} C_{11}^f & C_{12}^f & C_{13}^f & C_{14}^f & -C_{15}^f & -C_{16}^f \\ C_{12}^f & C_{22}^f & C_{23}^f & C_{24}^f & -C_{25}^f & -C_{26}^f \\ C_{13}^f & C_{23}^f & C_{33}^f & C_{34}^f & -C_{35}^f & -C_{36}^f \\ C_{14}^f & C_{24}^f & C_{34}^f & C_{44}^f & -C_{45}^f & -C_{46}^f \\ -C_{15}^f & -C_{25}^f & -C_{35}^f & -C_{45}^f & C_{55}^f & C_{56}^f \\ -C_{16}^f & -C_{26}^f & -C_{36}^f & -C_{46}^f & C_{56}^f & C_{66}^f \end{bmatrix} \quad (7)$$

Now that the four subcell stiffness matrices are computed, they need to be combined in order to arrive at a single stiffness matrix for the RVC. The transformed subcell stiffness matrices are next homogenized in order to obtain the effective material properties of the RVC.

Downloaded by GEORGIA INST OF TECHNOLOGY on January 25, 2014 | http://arc.aiaa.org | DOI: 10.2514/6.2014-0631

III. Homogenization Method

The homogenization procedure used by Ivanov and Tabiei was formulated in an earlier work[13]. Iso-stress and strain conditions are assumed across the subcell boundaries. The strain and strain components are divided into the iso-strain or in-plane components and the iso-stress or out-of-plane components. The subcell 6 component stress and strain vectors are expressed using the organizational convention in (1). These components are reorganized to group the in-plane and out-of-plane components together. The three in-plane stress components expressed in the RVC coordinate system are organized as follows, as a function of both the in plane and out of plane strain components.

$$\{\sigma_N\}_k = \begin{Bmatrix} \sigma_{XX} \\ \sigma_{YY} \\ \sigma_{XY} \end{Bmatrix}_k = \begin{bmatrix} C_{11} & C_{12} & C_{14} \\ C_{21} & C_{22} & C_{24} \\ C_{41} & C_{42} & C_{44} \end{bmatrix}_k \begin{Bmatrix} \varepsilon_{XX} \\ \varepsilon_{YY} \\ \gamma_{XY} \end{Bmatrix}_k + \begin{bmatrix} C_{13} & C_{15} & C_{16} \\ C_{23} & C_{25} & C_{26} \\ C_{43} & C_{45} & C_{46} \end{bmatrix}_k \begin{Bmatrix} \varepsilon_{ZZ} \\ \gamma_{YZ} \\ \gamma_{XZ} \end{Bmatrix}_k \tag{8}$$

The subscript (*N*) denotes the iso-strain or in plane components. These are the stress and strain components associated with plane stress conditions. The (*k*) subscript is used to denote the subcells (*f, w, F,W*). A contracted notation is used for the remainder of the formulation.

$$\{\sigma_N\}_k = [C_{NN}]_k \{\varepsilon_N\}_k + [C_{NS}]_k \{\varepsilon_S\}_k \tag{9}$$

The subscript (*S*) denotes the iso-stress or out-of-plane components.The three out-of-plane stress components expressed in the RVC coordinate system are organized as follows, as a function of both the in-plane and out-of-plane strain components.

$$\{\sigma_S\}_k = \begin{Bmatrix} \sigma_{ZZ} \\ \sigma_{YZ} \\ \sigma_{XZ} \end{Bmatrix}_k = \begin{bmatrix} C_{31} & C_{32} & C_{34} \\ C_{51} & C_{52} & C_{54} \\ C_{61} & C_{62} & C_{64} \end{bmatrix}_k \begin{Bmatrix} \varepsilon_{XX} \\ \varepsilon_{YY} \\ \gamma_{XY} \end{Bmatrix}_k + \begin{bmatrix} C_{33} & C_{35} & C_{36} \\ C_{53} & C_{55} & C_{56} \\ C_{63} & C_{65} & C_{66} \end{bmatrix}_k \begin{Bmatrix} \varepsilon_{ZZ} \\ \gamma_{YZ} \\ \gamma_{XZ} \end{Bmatrix}_k \tag{10}$$

Similar to the iso-strain components, the contracted notation is a follows:

$$\{\sigma_S\}_k = [C_{SN}]_k \{\varepsilon_N\}_k + [C_{SS}]_k \{\varepsilon_S\}_k \tag{11}$$

The result of the homogenization procedure is the effective stiffness matrix shown below. The effective stress components are constructed using volumetric averages of the subcells known as the rule of mixture. This is permitted by assuming that at all points, within the homogenized volume, the stress and strain are the same.

$$\begin{Bmatrix} \overline{\sigma}_N \\ \overline{\sigma}_S \end{Bmatrix} = \{\overline{\sigma}\} = [\overline{C}']\{\overline{\varepsilon}\} = \begin{bmatrix} \overline{C}_{NN} & \overline{C}_{NS} \\ \overline{C}_{SN} & \overline{C}_{SS} \end{bmatrix} \begin{Bmatrix} \overline{\varepsilon}_N \\ \overline{\varepsilon}_S \end{Bmatrix} \tag{12}$$

Applying the mixed boundary conditions to the subcells, the iso-strain assumption implies that the effective in-plane strains must be the same across the subcells. In addition, the out-of-plane stresses are also assumed to be the same.

$$\{\overline{\varepsilon}_N\} = \{\varepsilon_N\}_k \tag{13}$$

$$\{\overline{\sigma}_S\} = \{\sigma_S\}_k \tag{14}$$

The rule of mixtures is applied to the out-of-plane strains and the in-plane stresses.

Downloaded by GEORGIA INST OF TECHNOLOGY on January 25, 2014 | http://arc.aiaa.org | DOI: 10.2514/6.2014-0631

$$\{\bar{\varepsilon}_S\} = \sum_k f_k \{\varepsilon_S\}_k \tag{15}$$

$$\{\bar{\sigma}_N\} = \sum_k f_k \{\sigma_N\}_k \tag{16}$$

The boundary conditions are associated with the shell or membrane element formulation. The volume fraction, f_k, of the k[th] subcell in the RVC can be varied to account for an unbalanced fabric. Using a value of (f_k = ¼) implies that the warp and fill yarns constitute equal portions of the RVC.

Substituting (13) and (14) into both (9) and (11) results in subcell out-of-plane strains and in-plane stresses expressed as a function of effective out-of-plane stresses and in-plane strains. These resulting quantities are then substituted into (15) and (16); which are then rearranged to arrive at the following equations, where the effective stresses are a function of the effective strains. For brevity, the math operation to arrive at these equations are forgone as the original derivation includes more detail[10].

$$\{\bar{\sigma}_N\} = \left(\left[C_1^*\right] + \left[C_2^*\right]\left[C_3^*\right]^{-1}\left[C_4^*\right]\right)\{\bar{\varepsilon}_N\} + \left(\left[C_2^*\right]\left[C_3^*\right]^{-1}\right)\{\bar{\varepsilon}_S\} \tag{17}$$

$$\{\bar{\sigma}_S\} = \left(\left[C_3^*\right]^{-1}\left[C_4^*\right]\right)\{\bar{\varepsilon}_N\} + \left(\left[C_3^*\right]^{-1}\right)\{\bar{\varepsilon}_S\} \tag{18}$$

Where, intermediate matrices are defined below to condense the equations:

$$\begin{aligned}
\left[C_1^*\right] &= \sum_k f_k \left(\left[C_{NN}\right]_k - \left[C_{NS}\right]_k \left[C_{SS}\right]_k^{-1} \left[C_{SN}\right]_k\right) \\
\left[C_2^*\right] &= \sum_k f_k \left[C_{NS}\right]_k \left[C_{SS}\right]_k^{-1} \\
\left[C_3^*\right] &= \sum_k f_k \left[C_{SS}\right]_k^{-1} \\
\left[C_4^*\right] &= \sum_k f_k \left[C_{SS}\right]_k^{-1} \left[C_{SN}\right]_k
\end{aligned} \tag{19}$$

The effective stiffness matrix components are now defined from (12) using (17) and (18).

$$\begin{aligned}
\left[\bar{C}_{NN}\right] &= \left[C_1^*\right] + \left[C_2^*\right]\left[C_3^*\right]^{-1}\left[C_4^*\right] \\
\left[\bar{C}_{NS}\right] &= \left[C_2^*\right]\left[C_3^*\right]^{-1} \\
\left[\bar{C}_{SN}\right] &= \left[C_3^*\right]^{-1}\left[C_4^*\right] \\
\left[\bar{C}_{SS}\right] &= \left[C_3^*\right]^{-1}
\end{aligned} \tag{20}$$

The resulting effective stiffness matrix represents the properties of the fabric material expressed in the RVC coordinate system. The components of this matrix will be symmetric about the main diagonal due to the nature of the subcells. It should also be noted that the effective stiffness was reordered back to the original convention established prior to the homogenization process.

Downloaded by GEORGIA INST OF TECHNOLOGY on January 25, 2014 | http://arc.aiaa.org | DOI: 10.2514/6.2014-0631

$$\{\bar{\sigma}\} = \begin{Bmatrix} \bar{\sigma}_{XX} \\ \bar{\sigma}_{YY} \\ \bar{\sigma}_{ZZ} \\ \bar{\sigma}_{XY} \\ \bar{\sigma}_{YZ} \\ \bar{\sigma}_{XZ} \end{Bmatrix} = \begin{bmatrix} \bar{C}_{11} & \bar{C}_{12} & \bar{C}_{13} & \bar{C}_{14} & 0 & 0 \\ \bar{C}_{21} & \bar{C}_{22} & \bar{C}_{23} & \bar{C}_{24} & 0 & 0 \\ \bar{C}_{31} & \bar{C}_{32} & \bar{C}_{33} & \bar{C}_{34} & 0 & 0 \\ \bar{C}_{41} & \bar{C}_{42} & \bar{C}_{43} & \bar{C}_{44} & 0 & 0 \\ 0 & 0 & 0 & 0 & \bar{C}_{55} & \bar{C}_{56} \\ 0 & 0 & 0 & 0 & \bar{C}_{65} & \bar{C}_{66} \end{bmatrix} \begin{Bmatrix} \bar{\varepsilon}_{XX} \\ \bar{\varepsilon}_{YY} \\ \bar{\varepsilon}_{ZZ} \\ \bar{\gamma}_{XY} \\ \bar{\gamma}_{YZ} \\ \bar{\gamma}_{XZ} \end{Bmatrix} \tag{21}$$

A final coordinate system is defined to account for possible fabric orientations related to applied loads. In the (*X*,*Y*,*Z*) or RVC coordinate system, loading along the X axis is equivalent to loading the plain-weave in the bias direction. It is often desirable to load along the yarn directions. Thus, a second transformation is made to express the fabric stiffness matrix in the axis in which loading is applied. The rotation angle is defined as follows from the angle, α, which is set as an initial condition similar to θ, β_f, and β_w.

$$\delta = \alpha - \theta \tag{22}$$

The effective stiffness matrix is arrived at using the following transformation. Several angles have been defined between the three coordinate systems, so Figure 4 can be used to visually represent the coordinate systems on the RVC. This figure contains directional unit vectors and angles that are presented in the next section.

$$\left[\bar{C}\right] = \left[T(\delta)\right]^{-T}\left[\bar{C}'\right]\left[T(\delta)\right]^{-1} \tag{23}$$

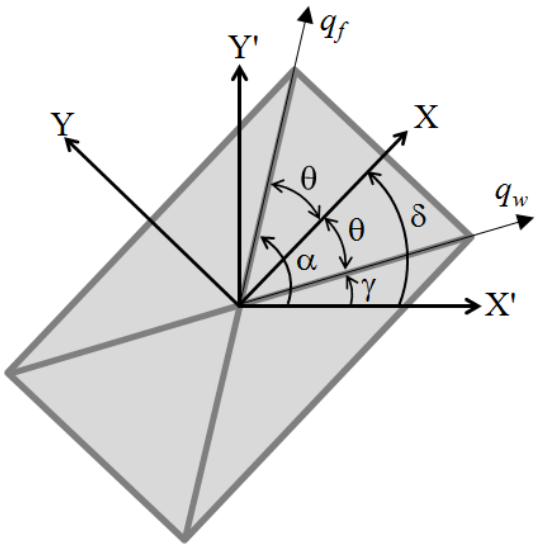

Figure 4: Orientation of Yarns in RVC

Since the resulting model is implemented in a plane element , only the components associated with the in-plane components of the matrix is necessary. The reduced stiffness matrix is used to calculate an increment in stress due to an increment in strain at each pseudo timestep of the non-linear finite element analysis code.

$$\begin{Bmatrix} \bar{\sigma}_{XX'} \\ \bar{\sigma}_{YY'} \\ \bar{\sigma}_{XY'} \end{Bmatrix} = \begin{bmatrix} \bar{C}_{11} & \bar{C}_{12} & \bar{C}_{13} \\ \bar{C}_{21} & \bar{C}_{22} & \bar{C}_{23} \\ \bar{C}_{31} & \bar{C}_{32} & \bar{C}_{33} \end{bmatrix} \begin{Bmatrix} \bar{\varepsilon}_{XX'} \\ \bar{\varepsilon}_{YY'} \\ \bar{\gamma}_{XY'} \end{Bmatrix} \tag{24}$$

IV. Yarn Reorientation

The reorientation of the fabric yarns is accounted for in this model. At a given pseudo time step, the current state of the finite element model is a function of the yarns in the RVC. Geometric nonlinearity is introduced to the model through the yarn reorientation and possible locking. To account for this, a geometric nonlinear analysis code is implemented in MATLAB. A simple strain controlled incremental approach using constant pseudo time step increments is employed. As shown in Figure 4, unit direction vectors q_f and q_w are defined in the (*X'*,*Y'*,*Z'*) coordinate system for the fill and warp yarns, respectively. The unit direction vectors for the warp and fill yarns are defined for the yarn material in the *w* and *f* subcells. Initially, the unit direction vectors are defined as follows:

$$\{q_f\} = \{\cos\beta_f \cos\alpha \quad \cos\beta_f \sin\alpha \quad \sin\beta_f\}^T \tag{25}$$

Downloaded by GEORGIA INST OF TECHNOLOGY on January 25, 2014 | http://arc.aiaa.org | DOI: 10.2514/6.2014-0631

$$\{q_w\} = \{\cos\beta_w \cos\gamma \quad \cos\beta_w \sin\gamma \quad \sin\beta_w\}^T \tag{26}$$

Where the angle γ is defined on the RVC and is calculated as follows:

$$\gamma = \alpha - 2\theta \tag{27}$$

The deformation gradient matrix, [*F*], is used to update the unit direction vectors at each pseudo time step. Due to the small increments in strain, an infinitesimal strain assumption is employed to construct the deformation gradient from the strain increment vector as follows:

$$[F] = \begin{bmatrix} 1+\Delta\bar{\varepsilon}_{XX} & \Delta\bar{\varepsilon}_{XY}/2 & 0 \\ \Delta\bar{\varepsilon}_{XY}/2 & 1+\Delta\bar{\varepsilon}_{YY} & 0 \\ 0 & 0 & 1+\Delta\bar{\varepsilon}_{ZZ} \end{bmatrix} \tag{28}$$

Using the deformation gradient matrix, the unit direction vectors can be updated as follows:

$$\{q_f^*\} = [F]\{q_f\} \quad and \quad \{q_w^*\} = [F]\{q_w\} \tag{29}$$

$$\{q_f\} = \{q_f^*\} / \|\{q_f^*\}\| \quad and \quad \{q_w\} = \{q_w^*\} / \|\{q_w^*\}\| \tag{30}$$

The components of the updated unit direction vectors are used to update the material angles for the next time step:

$$\beta_f = \sin^{-1} q_{f3} \quad and \quad \beta_w = \sin^{-1} q_{w3} \tag{31}$$

$$\alpha = \tan^{-1}\left(q_{f2}/q_{f1}\right) \quad and \quad \gamma = \tan^{-1}\left(q_{w2}/q_{w1}\right) \tag{32}$$

$$\theta = (\alpha - \gamma)/2 \quad and \quad \delta = \alpha - \theta \tag{33}$$

For an explicit finite element code, such as LS-DYNA, the time integration stability conditions require small time steps. This works well with the infinitesimal strain assumption. In this work, a static finite element code is utilized with an incremental approach. Small increments are used to not violate the infinitesimal strain assumption.

The primary mechanism for transitioning the fabric from a trellis behavior, prior to locking, to an continuous medium after locking, is the discount factor, μ. Since this model is implemented in a static solver, a piecewise function, as defined below, suffices without inducing oscillation that might occur in a dynamic solver. A locking angle is used to calculate the discount factor and can be determined by the geometry of the woven fabric.

$$\mu = \begin{cases} 1 & if \quad \theta < \pi/4 - \theta_{LOCK} \\ \mu_0 & if \quad \theta \in \left(\pi/4 + \theta_{LOCK}\ ,\ \pi/4 + \theta_{LOCK}\right) \\ 1 & if \quad \theta > \pi/4 + \theta_{LOCK} \end{cases} \tag{34}$$

Downloaded by GEORGIA INST OF TECHNOLOGY on January 25, 2014 | http://arc.aiaa.org | DOI: 10.2514/6.2014-0631

V. Nonlinear Finite Element Analysis

The Mesomechanical material model presented above was implemented in MATLAB within a simple nonlinear analysis code that parallels that in Crisfield[14]. Nonlinear solution algorithms and basic plane elements are employed to understand this state-of-the-art material model. Planar 4-node isoparametric quadrilateral elements are sufficient for evaluating the model when subjected to in-plane loading.

The 2nd Piola-Kirchhoff (PKII) stress and Green's strain measures are used in this solver. Use of PKII stress and Green's strain is quite natural for problems involving large displacements and/or rotations. This is because PKII stress and Green's strain are invariant to rigid body rotations.

Using the incremental strains, the stresses at the integration points of the quad element are calculated as follows:

$$\{\Delta\bar{\sigma}\} = [\bar{C}]\{\Delta\bar{\varepsilon}\} \quad and \quad \{\bar{\sigma}\}^{n+1} = \{\bar{\sigma}\}^{n} + \{\Delta\bar{\sigma}\} \tag{35}$$

As seen in (28), the deformation gradient matrix requires the normal transverse strain increment. Because a plane element formulation is used, the normal transverse strain component is neglected. Thus, it must be calculated before the deformation gradient can be updated at the next time step. The following equation comes from the rotated form of (21) and assuming the stress in the normal transverse direction is zero.

$$\{\Delta\bar{\varepsilon}_{ZZ}\} = -\left(\bar{C}_{13}\Delta\bar{\varepsilon}_{XX} + \bar{C}_{23}\Delta\bar{\varepsilon}_{YY} + \bar{C}_{34}\Delta\bar{\varepsilon}_{XY}\right)/\bar{C}_{44} \tag{36}$$

VI. Numerical Results

A simple in-plane uniaxial loading example is presented below. This is a first step to assessing the model's capabilities. Future examples can include more complicated loading and geometry. This example demonstrates the load-deformation behavior of the fabric material in two different RVC orientations; uniaxial tension in the yarn direction (0° from the loading direction) and in the bias direction (45° from the loading direction). A simple rectangular sample is modeled using 4-node elements. The sample is 400×100×1 mm. The authors of this model note that the thickness is not the actual fabric thickness, but a thickness obtained by dividing the area density of the material by the mass density. This is done because the fabric is not a continuous medium.

Table 1: Material Data

Parameter	Value
E_1	74 GPa
E_2	7.4 GPa
G_{12}	2.5 GPa
G_{23}	5.0 GPa
ν_{12}	0.2
ν_{23}	0.2
β_f	1°
β_w	1°
θ_{lock}	10°
f	0.25
μ_0	1e-5
θ_0	45°

A consequence to using this RVC method is that the finite element mesh size must approximate the size of the RVC; therefore a mesh convergence study was foregone. A 40×10 mesh is assumed to be the appropriate size for the sample. The ends of the rectangular sample are constrained to simulate the clamped conditions experienced in experimental testing. In both cases (0° and 45°), one end of the model is incrementally displaced to 100 mm. The properties used in this example are provided in Table 1. These properties are somewhat arbitrary as there is no experimental data for validation purposes.

The stress-strain curves for the different orientations are shown Figure 5. As stress and strain vary throughout the model, the results shown are from an element close to the center of the sample. When the tension is applied along the yarn direction, the response is esstentially linear. However, loading in the bias direction results in a bi-linear stress-strain response. The slope for loading in the bias direction is low prior to locking, but transitions quickly to a steeper slope; more so than the sample loaded in the yarn direction after locking. With the yarns jammed together, the RVC effectively has two yarns nearly in line with the load direction.

The deformed finite element meshes are compared against the undeformed mesh in Figure 6. There is significantly more contraction in the transverse direction for the bias orientation. The trellis behavior causes the yarns to rotate a large amount prior to locking. These results are similar to what has been seen in experimental testing.

Downloaded by GEORGIA INST OF TECHNOLOGY on January 25, 2014 | http://arc.aiaa.org | DOI: 10.2514/6.2014-0631

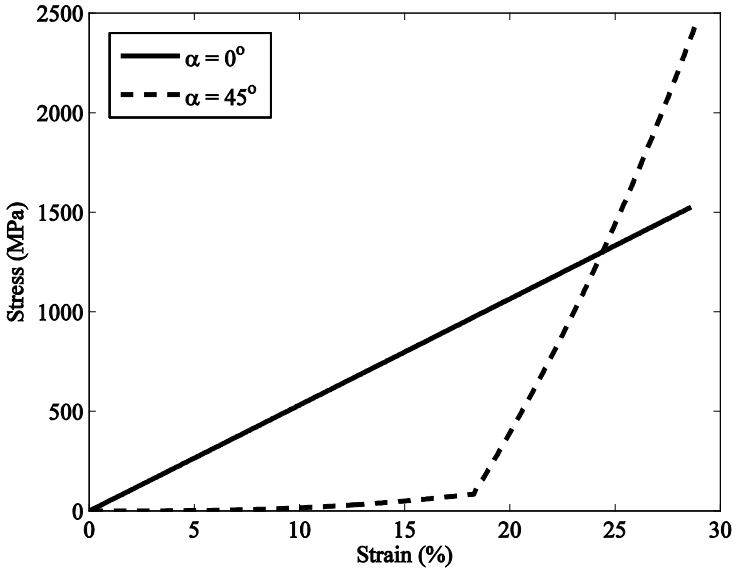

Figure 5: Material Behavior in Different Directions of Loading

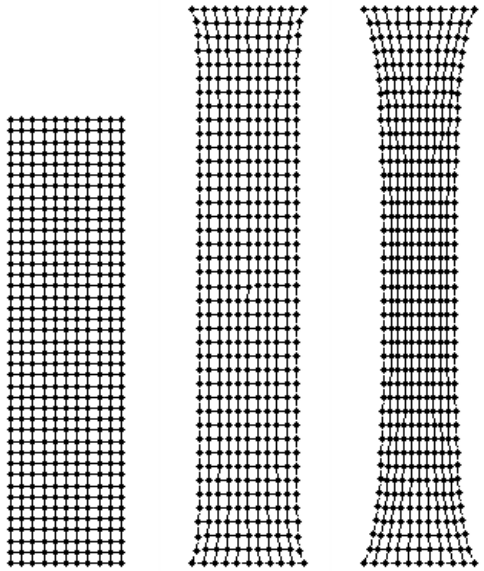

Figure 6: Initial Mesh (Left), 0° Orientation (Middle), 45° Orientation (Right)

VII. Summary and Future Work

The explored mesomechanical material model of a plain woven fabric was shown to be capable of capturing the dual behavior corresponding to that of actual fabrics. Simulations replicating actual tests for the normal and shear properties of fabrics show the trellising behavior before yarn locking followed by the elastic behavior of the fabric after locking. The model shows potential to obtain good agreement with experimental test data by varying the input parameters. Future work with this MATLAB model will include material data sensitivity analyses, comparisons to traditional material models, and inclusion of more complicated geometry and loading conditions.

Downloaded by GEORGIA INST OF TECHNOLOGY on January 25, 2014 | http://arc.aiaa.org | DOI: 10.2514/6.2014-0631

References

[1]Braun, R.D. and Manning, R.M., "Mars Exploration Entry, Descent, and Landing Challenges," Journal of Spacecraft and Rockets, vol. 44, no. 2, pp. 310-323, March-April 2007.

[2]Clark, I.G., Hutchings, A.L., Tanner, C.L., Braun, R.D., "Supersonic Inflatable Aerodynamic Decelerators for Use on Future Robotic Missions to Mars," *Journal of Spacecraft and Rockets*, Vol. 46, No. 2, 2009, pp. 340-352.

[3]Coatta, D., "Development and Testing of an 8 Meter Isotensoid Supersonic Inflatable Aerodynamic Decelerator," AIAA 2013-1328, 22nd AIAA Aerodynamic Decelerator Systems Technology Conference, Daytona Beach, FL, March 2013

[4]Clark I.G., "Aerodynamic Design, Analysis, and Validation of a Supersonic Inflatable Decelerator," Ph.D. Dissertation, Daniel Guggenheim School of Aerospace Engineering, Georgia Institute of Technology, Atlanta, GA, 2009.

[5]Lichodziejewski, L., "Ground and Flight Testing of a Stacked Tori Hypersonic Inflatable Aerodynamic Decelerator Configuration," AIAA 2011-1864, 54nd Structures, Structural Dynamics, and Materials Conference, Boston, MA, April 2013

[6]Hutchings, A.L., Braun, R.D., Masuyama, K., and Welch, J.V., "Experimental Determination of Material Properties for Inflatable Aeroshell Structures," AIAA Paper 2009-2949, 2009.

[7]Hill, J.L.; and Braun, R.D.;"Implementation of a Mesomechanical Material Model for IAD Fabrics within LS-DYNA," AIAA 2013-1367, 22nd AIAA Aerodynamic Decelerator Systems Technology Conference, Daytona Beach, FL, March 2013

[8]Murman, S.M., Suresh, S.S., "Modeling Effective Stiffness Properties of IAD Fabrics," AIAA 2011-2568

[9]Peng, X.Q., Cao, J., "Numerical Determination of Mechanical Elastic Constants of Textile Constants," 15th Annual Technical Conference of the American Society for Composite, College Station TX, Sept. 25-27, 2000

[10]Tabiei, A., Ivanov I., "Computational Micro-Mechanical Model of Flexible Woven Fabric for Finite Element Impact Simulation," 7th International LS-DYNA Users Conference, 2001

[11]Cavallaro, P.V., Johnson, M.E., Sadegh, A.M., "Mechanics of Plain-Woven Fabrics for Inflated Structures," Composite Structures, Vol. 61, 2003, pp. 375-393

[12]Cook, R.D., Malkus, D.S., Plesha, M.E., Concepts and Applications of Finite Element Analysis, 3rd ed., Wiley, NY, 1989

[13]Karayaka, M., Kurath, P., "Deformation and Failure Behavior of Woven Composites Laminates", J. Eng. Mater. Technol., Vol. 116, pp. 222-232, 1994

[14]Crisfield, M. A., "Non-linear Finite Element Analysis of Solids and Structures," New York, NY, John Wiley & Sons, 1991.

Downloaded by GEORGIA INST OF TECHNOLOGY on January 25, 2014 | http://arc.aiaa.org | DOI: 10.2514/6.2014-0631